Zornberg, J.G., and Li, C. (2003). "Design of Fiber-Reinforced Soil." Proceedings of the *Twelfth Panamerican Conference of Soil Mechanics and Geotechnical Engineering,* Cambridge, Massachusetts, June 22-26 Vol. 2, pp. 2193-2200.

Design of Fiber-reinforced Soil
Diseño de Suelo Reforzado con Fibras

Jorge G. Zornberg
University of Colorado at Boulder, USA
Chunling Li
University of Colorado at Boulder, USA

Abstract

The objective of this study is to experimentally validate a discrete methodology for the design of fiber-reinforced soil. The analysis of fiber-reinforced soil using a discrete approach can be conducted by independent characterization of soil specimens and of fiber specimens since the contributions of soil and fibers are treated separately. The fiber-induced distributed tension is a function of the volumetric fiber content, interface shear strength, and fiber aspect ratio when failure is induced by pullout of individual fibers. An experimental testing program involving triaxial testing of unreinforced and fiber-reinforced specimens was undertaken to validate the discrete methodology. As predicted by the analytical framework, the experimental results verify that the fiber-induced distributed tension is proportional to the fiber content and fiber aspect ratio when failure occurs by pullout of individual fibers. This proportionality is also observed for the stress-strain response of the fiber-reinforced specimens.

Resumen

Este estudio tiene por objetivo validar experimentalmente una metodología discreta para el diseño de suelo reforzado con fibras. El análisis de suelo reforzado con fibras usando un enfoque discreto puede ser conducido caracterizando muestras de suelo y muestras de fibra independiente porque las contribuciones de suelo y fibras son tratado separadamente. La tensión distribuida inducida por las fibras cuando ruptura es inducida por arrancamiento de las fibras es función del contenido de volumétrico de fibra, la resistencia al corte de las interfaces, y la razón del aspecto de fibra. Un programa experimental consistente en ensayos triaxiales de especimenes tanto no reforzados cuanto reforzados fue emprendido para validar la metodología discreta. Consistente con la predicción analítica, los resultados experimentales verifican que la tensión distribuida inducida de fibra es proporcional al contenido de fibra y a la razón del aspecto de fibra cuando la ruptura ocurre por arrancamiento. Esta proporcionalidad es observada también en la respuesta tension-deformación de los especimenes reforzados con fibra

1 INTRODUCTION

Slope stabilization projects can involve either fiber-reinforcement or continuous planar reinforcement. Randomly distributed fibers over continuous inclusions can maintain strength isotropy and avoid the existence of the potential planes of weakness that can develop parallel to continuous planar reinforcement elements. Fiber reinforcement has become a promising solution to the stabilization of thin soil veneers and localized repair of failed slopes.

The design of fiber-reinforced soil slopes has typically been performed using composite approaches, where the fiber-reinforced soil is considered a single homogenized material. Accordingly, fiber-reinforced soil design has required non-conventional laboratory testing of composite fiber-reinforced soil specimens.

Several composite models have been proposed to explain the behavior of randomly distributed fibers within a soil mass. The proposed models have been based on mechanistic approaches (Maher and Gray, 1990), on energy dissipation approaches (Michalowski and Zhao, 1996), and on statistics-based approaches (Ranjan et al., 1996). The mechanistic models proposed by Gray and Ohashi (1983) and Maher and Gray (1990) quantify the "equivalent shear strength" of the fiber-reinforced composite as a function of the thickness of the shear band that develops during

failure. Information needed to characterize shear band development for these models is, however, difficult to quantify (Shewbridge and Sitar, 1990). Common findings from the various testing programs implemented to investigate composite models include: (i) randomly distributed fibers provide strength isotropy in a soil composite; (ii) fiber inclusions increase the "equivalent" shear strength within a reinforced soil mass; and (iii) the "equivalent" strength typically shows a bilinear behavior, which was experimentally observed by testing of comparatively weak fibers under a wide range of confining stresses.

A discrete approach for the design of fiber-reinforced soil slopes was recently proposed to characterize the contribution of randomly distributed fibers to stability (Zornberg, 2002). In this approach, fiber-reinforced soil is characterized as a two-component (soil and fibers) material. The proposed methodology treats the fibers as discrete elements that contribute to stability by mobilizing tensile stresses along the shear plane. Consequently, independent testing of soil specimens and of fiber specimens, but not of fiber-reinforced soil specimens, can be used to characterize fiber-reinforced soil performance. Avoiding testing of fiber-reinforced soil specimens is a major objective of the proposed approach since the need of testing composite specimens in design has discouraged implementation of fiber-reinforcement in engineering practice.

This paper initially reviews the main concepts of the discrete approach and subsequently validates the framework for design purposes.

2 DISCRETE FRAMEWORK FOR FIBER REINFORCEMENT

2.1 Background

The volumetric fiber content, χ, used in the proposed discrete framework is defined as:

$$\chi = \frac{V_f}{V} \tag{1}$$

where V_f is the volume of fibers and V is the control volume of fiber-reinforced soil.

The gravimetric fiber content, χ_w, typically used in construction specifications, is defined as:

$$\chi_w = \frac{W_f}{W_s} \tag{2}$$

where W_f is the weight of fibers and W_s is the dry weight of soil. Consistent with engineering practice, the dry weight of soil is used in the definition above instead of the dry weight of fiber-reinforced soil. The definition of gravimetric fiber content is analogous to the classic definition of gravimetric moisture content.

The dry unit weight of the fiber-reinforced soil composite, γ_d, is defined as:

$$\gamma_d = \frac{W_f + W_s}{V} \tag{3}$$

The contribution of fibers to stability leads to an increased shear strength of the "homogenized" composite reinforced mass. However, the reinforcing fibers actually work in tension and not in shear. A major objective of the discrete framework is to explicitly quantify the fiber-induced distributed tension, t, which is the tensile force per unit area induced in a soil mass by randomly distributed fibers. Specifically, the magnitude of the fiber-induced distributed tension is defined as a function of properties of the individual fibers. In this way, as in analysis involving planar reinforcements, limit equilibrium analysis of fiber-reinforced soil can explicitly account for tensile forces.

The interface shear strength of individual fibers can be expressed as:

$$f_f = c_{i,c} \cdot c + c_{i,\phi} \cdot \tan\phi \cdot \sigma_{n,ave} \tag{4}$$

where c and ϕ are the cohesive and frictional components of the soil shear strength and $\sigma_{n,ave}$ is the average normal stress acting on the fibers. The interaction coefficients, $c_{i,c}$ and $c_{i,\phi}$, commonly used in soil reinforcement literature for continuous planar reinforcement, is adopted herein to relate the interface shear strength to the shear strength of the soil. The interaction coefficients are defined as:

$$c_{i,c} = \frac{a}{c} \tag{5}$$

$$c_{i,\phi} = \frac{\tan\delta}{\tan\phi} \tag{6}$$

where a is the adhesive component of the interface shear strength between soil and the polymeric fiber, $\tan\delta$ is the frictional component.

The pullout resistance of a fiber of length l_f should be estimated over the shortest side of the two portions of a fiber intercepted by the failure plane. The length of the shortest portion of a fiber intercepted by the failure plane varies from zero to $l_f/2$. Statistically, the average embedment length of randomly distributed fibers, $l_{e,ave}$, can be analytically defined by:

$$l_{e,ave} = \frac{l_f}{4} \tag{7}$$

where l_f is total length of the fibers.

The average pullout resistance can be quantified along the average embedment length, $l_{e,ave}$, of all individual fibers crossing a soil control surface A. The ratio between the total cross sectional area of the fibers A_f and the control surface A is assumed to be defined by the volumetric fiber content χ. That is:

$$\chi = \frac{A_f}{A} \tag{8}$$

When failure is governed by the pullout of the fibers, the fiber-induced distributed tension, t_p, is defined as the average of the tensile forces inside the fibers over the control area A. Consequently, t_p can be estimated as:

$$t_p = \chi \cdot \eta \cdot \left(c_{i,c} \cdot c + c_{i,\phi} \cdot \tan\phi \cdot \sigma_{n,ave}\right) \tag{9}$$

where η is the aspect ratio defined as:

$$\eta = \frac{l_f}{d_f} \tag{10}$$

where d_f is the equivalent diameter of the fiber.

When failure is governed by the yielding of the fibers, the distributed tension, t_t , is determined from the tensile strength of the fiber:

$$t_t = \chi \cdot \sigma_{f,ult} \tag{11}$$

where $\sigma_{f,ult}$ is the ultimate tensile strength of the individual fibers.

The fiber-induced distributed tension t to be used in the discrete approach to account for the tensile contribution of the fibers in limit equilibrium analysis is:

$$t = \min\left(t_p, t_t\right) \tag{12}$$

The critical normal stress, $\sigma_{n,crit}$, which defines the change in the governing failure mode, is the normal stress at which failure occurs simultaneously by pullout and tensile breakage of the fibers. That is, the following condition holds at the critical normal stress:

$$t_t = t_p \tag{13}$$

An analytical expression for the critical normal stress can be obtained as follows:

$$\sigma_{n,crit} = \frac{\sigma_{f,ult} - \eta \cdot c_{i,c} \cdot c}{\eta \cdot c_{i,\phi} \cdot \tan\phi} \tag{14}$$

2.2 Equivalent shear strength of reinforced fiber composites

As in analyses involving planar inclusions, the orientation of the fiber-induced distributed tension should also be identified or assumed. Specifically, the fiber-induced distributed tension can be assumed to act: a) along the failure surface so that the discrete fiber-induced tensile contribution can be directly "added" to the shear strength contribution of the soil in a limit equilibrium analysis; b) horizontally, which would be consistent with design assumptions for reinforced soil structures using planar reinforcements; and c) in a direction somewhere between the initial fiber orientation (which is random) and the orientation of the failure plane.

This equivalent shear strength of fiber-reinforced specimens can be defined as a function of the fiber-induced distributed tension t, and the shear strength of the unreinforced soil, S:

$$S_{eq} = S + \alpha \cdot t = c + \sigma_n \tan\phi + \alpha \cdot t \tag{15}$$

where α is an empirical coefficient that accounts for the direction of fiber-induced distributed tension. If the fiber-induced distributed tension t is assumed to be parallel to the shear plane, the magnitude of the normal stress acting on the shear plane is not affected by the fiber-induced distributed tension t, and α is then equal to 1.

Depending on whether the mode of failure is fiber pullout or yielding, the equivalent shear strength can be derived by combining (9) or (11) with (15). It should be noted that the average normal stress acting on the fibers, $\sigma_{n,ave}$, does not necessarily equal the normal stress on the shear plane σ_n . For randomly distributed fibers, $\sigma_{n,ave}$ could be represented by the octahedral stress component. However, a sensitivity evaluation undertaken using typical ranges of shear strength parameters show that $\sigma_{n,ave}$ can be approximated by σ_n without introducing significant error.

Accordingly, the following expressions can be used to define the equivalent shear strength when failure is governed by fiber pullout:

$$S_{eq,p} = c_{eq,p} + \left(\tan\phi\right)_{eq,p} \cdot \sigma_n \tag{16}$$

$$c_{eq,p} = \left(1 + \alpha \cdot \eta \cdot \chi \cdot c_{i,c}\right) \cdot c \tag{17}$$

$$\left(\tan\phi\right)_{eq,p} = \left(1 + \alpha \cdot \eta \cdot \chi \cdot c_{i,\phi}\right) \cdot \tan\phi \tag{18}$$

Equivalently, the following expressions can be obtained to define the equivalent shear strength when failure is governed by tensile breakage of the fibers:

$$S_{eq,t} = c_{eq,t} + \left(\tan\phi\right)_{eq,t} \cdot \sigma_n \tag{19}$$

$$c_{eq,t} = c + \alpha \cdot \chi \cdot \sigma_{f,ult} \tag{20}$$

$$\left(\tan\phi\right)_{eq,t} = \tan\phi \tag{21}$$

The above expressions yield a bilinear shear strength envelope, which is shown in Figure 1.

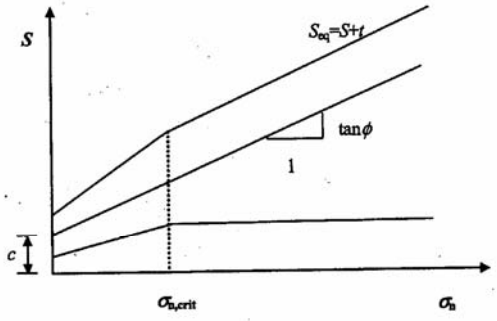

Figure 1 Representation of the equivalent shear strength according to the discrete approach

3 EXPERIMENTAL VALIDATION

3.1 Experimental testing program

A triaxial compression testing program on fiber-reinforced soil was implemented to validate the proposed discrete framework. The soils used classify as SP according to the USCS classification systems. The percentage of fines is approximately 1.4%.

The fibers used in the testing program were polypropylene fibers with linear densities of 360 and 1000 denier and fiber lengths of 25 mm and 50 mm. Both fibrillated fibers and tapes without the fibrillation were used. A series of tensile test were performed in general accordance with ASTM D2256-97 to evaluate the ultimate tensile strength of fibers. The average tensile strength of the fibers was approximately 425,000 kPa.

The triaxial testing program involved consolidated drained (CD) test. The unreinforced tests yielded an effective shear strength envelope defined by cohesion of 6.1 kPa and friction angle of 34.3°. The soils were reinforced using gravimetric fiber contents of 0.2% and 0.4%.

The governing failure mode for the polymeric fibers used in this investigation is pullout because of the comparatively high tensile strength and comparatively short length of the fibers. Accordingly, the triaxial testing program conducted in this study focuses only on the first portion of the bilinear strength envelope shown in Figure 1.

3.2 Stress-strain behavior

Figure 2 shows the stress-strain behavior of specimens prepared using χ_w=0, 0.2 and 0.4 %. Specimens prepared using 360 denier fibers were tested under confining pressure of 70 kPa. The peak deviator stress increases approximately linearly with increasing fiber content, which is consistent with the discrete framework (see equation (9)). The post-peak shear strength loss is smaller in the reinforced specimens than in the unreinforced specimens. However, the initial portions of the stress-strain curves of the reinforced and unreinforced specimens are approximately similar. Accordingly, the soil appears to take most of the applied load at small strain levels, while the load resisted by the fibers is more substantial at higher strain level. The larger strain corresponding to the peak deviator stress displayed by the fiber-reinforced specimens suggests that fibers increase the ductility of the reinforced soil specimen. These findings are confirmed in Figure 3, which shows the test results obtained under higher confining stress (140 kPa).

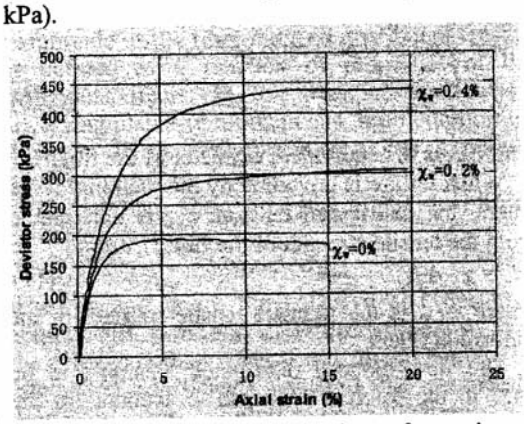

Figure 2 Stress-strain behavior of specimens prepared using χ_w=0, 0.2 and 0.4% with l_f =25 mm fibers (360 denier), σ_3=70 kPa

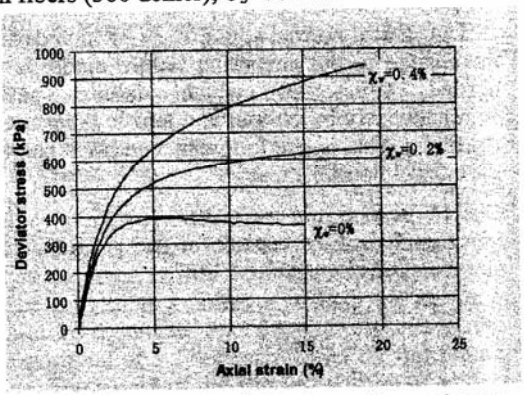

Figure 3 Stress-strain behavior of specimens prepared using χ_w=0, 0.2 and 0.4% with l_f =25 mm fibers (360 denier), σ_3=140kPa

The effect of fiber length on the stress-strain behavior is shown in Figure 4. The specimens

were prepared using fibers with a different fiber type (1000 denier) than that used in the tests shown in Figures 2 and 3. The specimens were prepared using the same gravimetric fiber content, but with varying fiber length. The specimens reinforced with longer (50 mm) fibers displayed higher shear strength. The peak deviator stress increases linearly with increasing aspect ratio, which is also consistent with the trend indicated by equation (9). The strain corresponding to the peak strength increases with increasing fiber length. When the governing failure mode is pullout, the fiber-induced distributed tension reaches its peak when the pullout resistance is fully mobilized. For longer fibers, it usually requires a larger interface shear deformation to fully mobilize the interface strength. Consequently, the macroscopic axial strain at peak stress should be larger for specimen reinforced with longer fibers. Figure 5 shows a similar trend for the case of tests conducted under higher confining pressures.

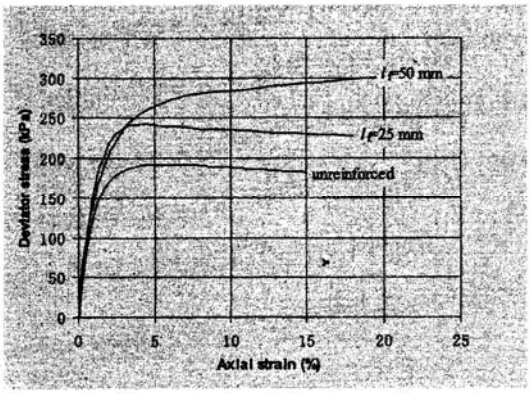

Figure 4 Stress-strain behavior of specimens prepared using χ_w=0.2%, with l_f=25 mm and 50 mm fibers (1000 denier), σ_3=70 kPa

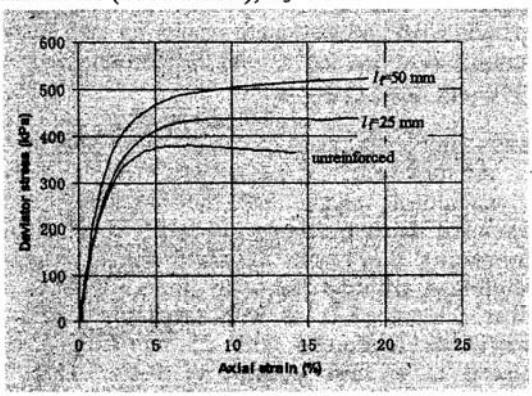

Figure 5 Stress-strain behavior of specimens prepared using χ_w=0.2%, with l_f=25 mm and 50 mm fibers (1000 denier), σ_3=140 kPa

3.3 Shear strength behavior

Equations (16) through (18) were used to predict the equivalent shear strength for fiber-reinforced specimens. Interaction coefficients of 0.8 are assumed in the analyses conducted in this study. The interface shear strength obtained from pullout test results conducted on woven geotextiles was considered representative of the interface shear strength on individual fibers. For practical purposes, interaction coefficients can be selected from values reported in the literature for continuous planar reinforcements. This is because pullout tests conducted using a variety of soils and planar geosynthetics have been reported to render interaction coefficient values falling within a narrow range (Koutsourais et al., 1998).

The effect of fiber content on shear strength is shown in Figure 6, which compares the experimental data and predicted shear strength envelopes obtained using 25 mm fibers placed at fiber contents of 0.0%, 0.2%, and 0.4%. Results obtained using 360 denier fibers are shown in the figure. The experimental results show a clear increase in equivalent shear strength with increasing fiber content. No major influence of fibrillation is perceived in the results of the testing program. The shear strength envelope for the unreinforced specimens was defined by fitting the experimental data. However, the shear strength envelopes shown in the figure for the reinforced specimens were predicted analytically using the proposed discrete framework. A very good agreement is observed between experimental data points and predicted shear strength envelopes. As predicted by the discrete framework, the distributed fiber-induced tension increases linearly with the volumetric fiber content. Similar observation can be made in Figure 7, which shows the results obtained using the same test conditions as those shown in Figure 6 but using 50 mm-long fibers.

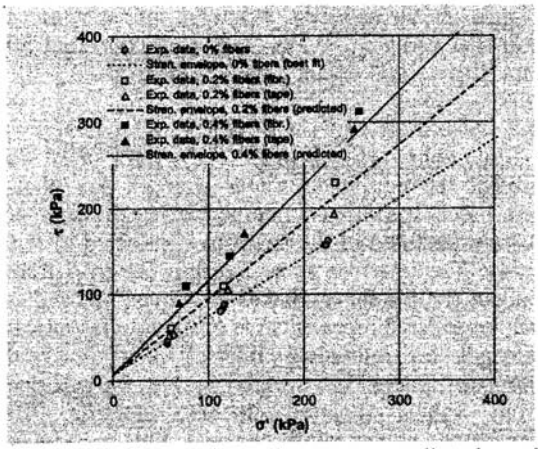

Figure 6 Comparison between predicted and experimental shear strength results for specimens reinforced at χ_w=0.0%, 0.2%, 0.4% with 25 mm-long fibers (360 denier)

The effect of fiber aspect ratio on shear strength is shown in Figure 8, which compares the experimental and predicted shear strength envelopes of specimens placed at χ_w=0.2%, with 25 and 50 mm-long fibers. As predicted by the discrete framework, increasing the fiber length increases the pullout resistance of individual fibers, and results in a higher fiber-induced distributed tension. Consequently, for the same fiber content, specimens reinforced with longer fibers will have higher equivalent shear strength. This trend agrees well with the experimental data. Similar observation can be made from Figure 9, which shows the results obtained using the same test conditions as those in Figure 8 but using χ_w=0.4%.

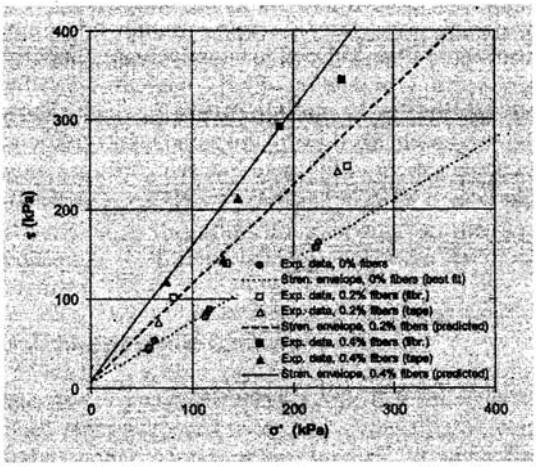

Figure 7 Comparison between predicted and experimental shear strength results for specimens reinforced at χ_w=0.0%, 0.2%, 0.4% with 25 mm-long fibers (360 denier)

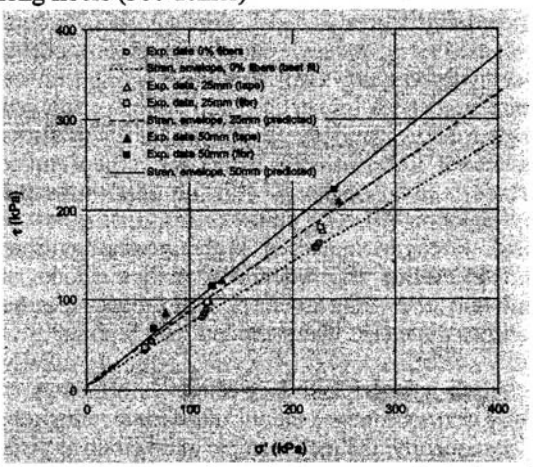

Figure 8 Comparison between predicted and experimental shear strength results for specimens reinforced at χ_w=0.2%, with 25 mm-long and 50 mm-long fibers (1000 denier)

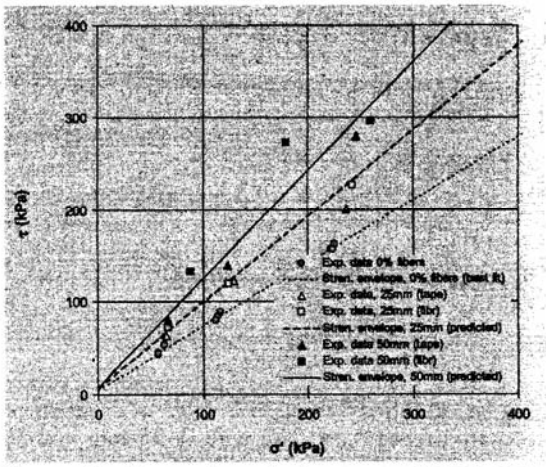

Figure 9 Comparison between predicted and experimental shear strength results for specimens reinforced at χ_w=0.4%, with 25 mm-long and 50 mm-long fibers (1000 denier)

3.4 Combined effect of aspect ratio and fiber content

Additional insight into the validity of the proposed discrete approach can be obtained by comparing the results obtained for specimens reinforced with 50 mm-long fibers placed at a fiber content of 0.2% with those obtained for specimens reinforced with 25 mm-long fibers placed at a fiber content of 0.4%. That is specimens with a constant value of $(\chi_w \cdot \eta)$. As inferred from inspection of equation (9) the fiber-

induced distributed tension is directly proportional to both the fiber content and the fiber aspect ratio. Consequently, the predicted equivalent shear strength parameters for the above combinations of fiber length and fiber content are the same. Figures 10 and 11 combine these experimental results.

The good agreement between experimental results and predicted values provides additional evidence of the suitability of the proposed discrete approach. From the practical standpoint, it should be noted that using 50 mm-long fibers placed at a fiber content of 0.2% corresponds to half the reinforcement material than using 25 mm-long fibers placed at a fiber content of 0.4%. That is, for the same target equivalent shear strength the first combination leads to half the material costs than the second one. It is anticipated, though, that difficulty in achieving good fiber mixing may compromise the validity of the relationships developed herein for comparatively high aspect ratios (i.e. comparatively long fibers) and for comparatively high fiber contents. The fiber content or fiber length at which the validity of these relationships is compromised should be further evaluated. Nonetheless, good mixing was achieved for the fiber contents and fiber lengths considered in this investigation, which were selected based on values typically used in geotechnical projects.

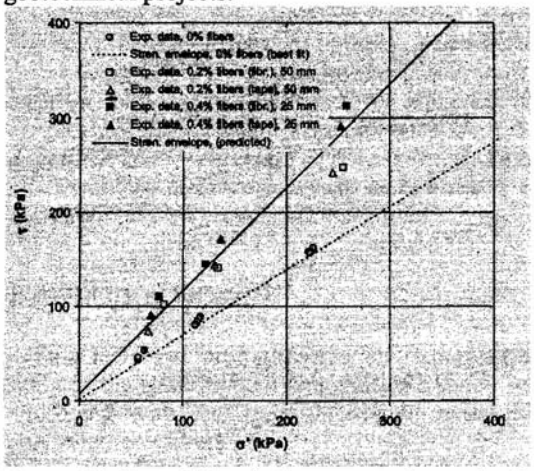

Figure 10 Consolidated shear strength results for specimen reinforced with 50mm-long fibers (360 denier) placed at χ_w=0.2% and 25 mm fibers placed at χ_w=0.4%

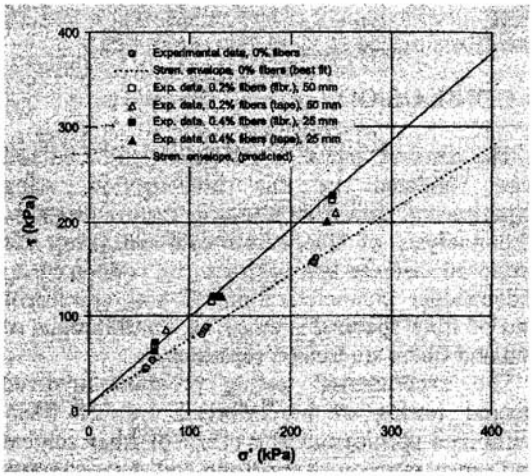

Figure 11 Consolidated shear strength results for specimen reinforced with 50 mm-long fibers (1000 denier) placed at χ_w=0.2% and 25 mm fibers placed at χ_w=0.4%

Figure 12 shows the stress-strain behavior of specimen reinforced with 50 mm fibers placed at χ_w=0.2% and 25 mm fibers placed at χ_w=0.4%. While the discrete approach was developed only to predict the shear strength response, the results in the figure show that fiber-reinforced specimens prepared using a constant value of ($\chi_w \cdot \eta$) display similar stress-strain behavior. This similar response is observed for both fibrillated and tape fibers, suggesting that the fibrillation procedure does not have a significant impact on the mechanical response of fiber-reinforced soil. The experimental results suggest that the proportionality of shear strength with the fiber content and fiber aspect ratio predicted by the discrete framework can be extrapolated to the entire stress-strain response of fiber-reinforced specimens.

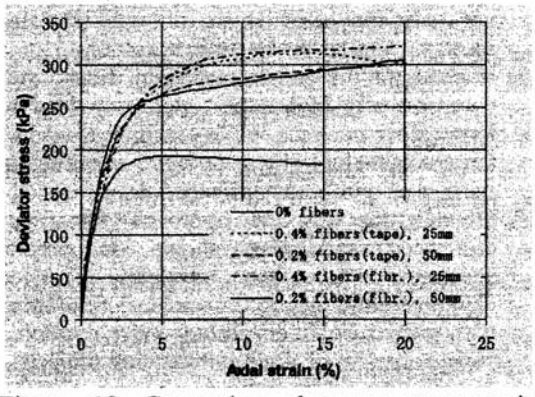

Figure 12 Comparison between stress-strain behavior for specimen reinforced with 50mm

fibers (1000 denier) placed at χ_w=0.2% and 25 mm fibers placed at χ_w=0.4%, σ_3=70 kPa

4 CONCLUSIONS

The discrete approach for fiber-reinforced soil was validated in this investigation using experimental data from a triaxial testing program. The analysis of fiber-reinforced soil using the proposed discrete approach can be conducted by independent characterization of soil specimens and of fiber specimens since the contributions of soil and fibers are treated separately.

The experimental testing program involved triaxial testing of unreinforced and of fiber-reinforced specimens. The effect of fiber content and aspect ratio on stress-strain and shear strength results was examined using the experimental results. In addition, the shear strength results were compared with the analytic predictions using the discrete framework. The main conclusions drawn from this investigation are:

(a) The addition of fibers can significantly increase the peak shear strength and limit the post peak strength loss of the soil. An increase in fiber content leads to increasing strain at failure and, consequently, to a more ductile behavior.

(b) The peak shear strength increases with increasing aspect ratio. The strain at peak deviator stress increases with increasing fiber aspect ratio

(c) As predicted by the discrete framework, the experimental results confirmed that the fiber-induced distributed tension increases linearly with fiber content and fiber aspect ratio when failure is characterized by pullout of individual fibers.

(d) Experimental results conducted using specimens with a constant ($\chi_w \cdot \eta$) value show not only the same shear strength but also display a similar stress-strain behavior.

(e) If good mixing can be achieved, fibers with comparatively high aspect ratio can lead to lower fiber contents while reaching the same target equivalent shear strength, resulting in savings of reinforcement material.

(f) Overall, the discrete approach for fiber-reinforced soil was shown to predict accurately the shear strength obtained experimentally using specimens reinforced with polymeric fibers tested under confining stresses typical of slope stabilization projects.

REFERENCES

Gray, D.H. and Al-Refeai, T. (1986). "*Behavior of Fabric versus Fiber-reinforced Sand*", ASCE J. Geotech. Engrg. 112(8): 804-820.

Gray, D.H. and Ohashi, H. (1983). "*Mechanics of Fiber-reinforcement in Sand*", ASCE J. Geotech. Engrg. 109(3): 335-353.

Gregory, G. H. and Chill, D. S. (1998). "*Stabilization of Earth Slopes with Fiber-reinforcement*", Proc. 6th Int. Conf. Geosynthetics, Atlanta, Georgia, March 1998, 1073-1078.

Koutsourais, M., Sandri, D., and Swan, R. (1998). "*Soil Interaction Characteristics of Geotextiles and Geogrids*". Proc. 6th Int. Conf. Geosynthetics, Atlanta, Georgia, March 1998, 739-744.

Maher, M.H. and Gray, D.H. (1990). "*Static Response of Sand Reinforced With Randomly Distributed Fibers*", ASCE J. Geotech. Engrg. 116(11): 1661-1677.

Michalowski, R.L. and Zhao, A. (1996). "*Failure of Fiber-Reinforced Granular Soils*". ASCE J. Geotech. Engrg. 122(3): 226-234.

Ranjan, G., Vassan, R.M. and Charan, H.D. (1996). "*Probabilistic Analysis of Randomly Distributed Fiber-Reinforced Soil*", ASCE J. Geotech. Engrg. 120(6): 419-426.

Shewbridge, S.E. and Sitar, N. (1990). "*Deformation Based Model for Reinforced Sand*", ASCE J. Geotechnical Engineering 116(7): 1153-1170.

Zornberg, J.G. (2002) "*Discrete framework for limit equilibrium analysis of fibre-reinforced soil*", Géotechnique 52(8): 593–604

SOIL AND ROCK AMERICA 2003

12th Panamerican Conference on Soil Mechanics and Geotechnical Engineering

12° Conferencia Panamericana de Mecánica de Suelos e Ingenieria Geotécnica

39th U.S. Rock Mechanics Symposium

June 22 - 26, 2003
Cambridge, Massachusetts, USA

PROCEEDINGS VOLUME 2

Edited by:

Patricia J. Culligan
Herbert H. Einstein
Andrew J. Whittle

Massachusetts Institute of Technology

VERLAG GLÜCKAUF GMBH · ESSEN (GERMANY) 2003